AD_____

Award Number: W81XWH-11-2-0125

TITLE: The Use of Inhibitors of Mechanosensitive Ion Channels as Local Inhibitors of Peripheral Pain

PRINCIPAL INVESTIGATOR: Frederick Sachs, Ph.D.

CONTRACTING ORGANIZATION: SUNY at Buffalo
Buffalo, NY 14214

REPORT DATE: March 2013

TYPE OF REPORT: Annual

PREPARED FOR: U.S. Army Medical Research and Materiel Command
Fort Detrick, Maryland 21702-5012

DISTRIBUTION STATEMENT: Approved for Public Release;
Distribution Unlimited

The views, opinions and/or findings contained in this report are those of the author(s) and should not be construed as an official Department of the Army position, policy or decision unless so designated by other documentation.

REPORT DOCUMENTATION PAGE

Form Approved
OMB No. 0704-0188

Public reporting burden for this collection of information is estimated to average 1 hour per response, including the time for reviewing instructions, searching existing data sources, gathering and maintaining the data needed, and completing and reviewing this collection of information. Send comments regarding this burden estimate or any other aspect of this collection of information, including suggestions for reducing this burden to Department of Defense, Washington Headquarters Services, Directorate for Information Operations and Reports (0704-0188), 1215 Jefferson Davis Highway, Suite 1204, Arlington, VA 22202-4302. Respondents should be aware that notwithstanding any other provision of law, no person shall be subject to any penalty for failing to comply with a collection of information if it does not display a currently valid OMB control number. **PLEASE DO NOT RETURN YOUR FORM TO THE ABOVE ADDRESS.**

1. REPORT DATE	2. REPORT TYPE	3. DATES COVERED
March 2013	Annual	25 February 2012 – 24 February 2013

4. TITLE AND SUBTITLE

The Use of Inhibitors of Mechanosensitive Ion Channels as Local Inhibitors of Peripheral Pain

5a. CONTRACT NUMBER

5b. GRANT NUMBER
W81XWH-11-2-0125

5c. PROGRAM ELEMENT NUMBER

6. AUTHOR(S)

Frederick Sachs, Thomas Suchyna, Phillip Gottlieb

E-Mail: sachs@buffalo.edu, mailto:suchyna@buffalo.edu, mailto:philgott@buffalo.edu

5d. PROJECT NUMBER

5e. TASK NUMBER

5f. WORK UNIT NUMBER

7. PERFORMING ORGANIZATION NAME(S) AND ADDRESS(ES)

SUNY at Buffalo
Buffalo, NY 14214

8. PERFORMING ORGANIZATION REPORT NUMBER

9. SPONSORING / MONITORING AGENCY NAME(S) AND ADDRESS(ES)
U.S. Army Medical Research and Materiel Command
Fort Detrick, Maryland 21702-5012

10. SPONSOR/MONITOR'S ACRONYM(S)

11. SPONSOR/MONITOR'S REPORT NUMBER(S)

12. DISTRIBUTION / AVAILABILITY STATEMENT
Approved for Public Release; Distribution Unlimited

13. SUPPLEMENTARY NOTES

14. ABSTRACT

This is a basic research project designed to understand the role of mechanically sensitive excitatory ion channels (MSC) in the pathology of chronic pain, and the use of a small peptide inhibitor of these channels called GsMTx4 to treatment peripheral pain. Our first goal is to develop an in vitro assay using single neurons to study the properties of MSCs and to determine the affinity of GsMTx4 and mutant analogs for neuronal MSCs. We have learned to prepare dorsal root ganglion neurons (DRG) from mouse spinal cord and have determined the types of MSCs expressed and the frequency of their occurrence in the cell-attached and outside-out patch assay. We have also designed a second assay for MSC activity by pressing on DRG with a precision controlled motion glass probe while measuring whole cell currents as a independent measure of the MSC activity. Stress on the internal cytoskeleton may play a critical role in the activation of MSCs on the surface and so we will measure stress changes in the proteins that make up the cytoskeleton of DRGs using a new FRET based stress probe we have made which can be inserted into the sequence of cytoskeletal proteins to report stress. We have tried to reproduce the published findings of others showing GsMTx4 analgesic activity in whole animals by treating inflamed tissue in mice, but were unable to do so. However, we have learned new information about the pharmacokinetics of GsMTx4 that will be used to redesign the study.

15. SUBJECT TERMS
None provided.

16. SECURITY CLASSIFICATION OF:			17. LIMITATION OF ABSTRACT	18. NUMBER OF PAGES	19a. NAME OF RESPONSIBLE PERSON
a. REPORT	b. ABSTRACT	c. THIS PAGE			USAMRMC
U	U	U	UU	22	19b. TELEPHONE NUMBER *(include area code)*

Table of Contents

Introduction: The focus of this grant is molecular mechanisms of mechanical transduction in dorsal root ganglia cells (DRGs) that are likely to give rise to the sensation of pain. The first goal was to understand how a specific peptide inhibitor of mechanosensitive ion channels (MSCs) acts to suppress transduction. This involves single channel patch clamp electrophysiology assays and the synthesis of mutant peptides to elaborate the contributions of specific molecular components. A second goal is to extend the single channel patch experiments to whole cell recording where the cytoskeleton is more intact. A third goal is understand how external mechanical stress is distributed in proteins of the cytoskeleton since those mechanics affect the stress in the lipid bilayer where the channels reside. Finally, if we arrive at some promising therapies based on *in vitro* data we will measure the analgesic effects of the peptides in intact mice or rats and correlate nociceptive sensitivity.

Body:

Aim 1) The goal of this aim is to synthesize mutants of GsMTx4 to determine amino acids important to the peptide interaction with MSCs and the membrane. This information could be used to modify the peptide to increase its inhibitory effect or to change its specificity for different MSCs. We are currently preparing the final version of a manuscript that will be submitted soon. The manuscript is a collaborative effort between our laboratory, which makes the actual current measurements and tests the different peptides mutants, and Dr. Kazu Nishizawa's laboratory at Teikyo University which does the molecular dynamic simulations used to predict GsMTx4 membrane interactions.

Lysines involved in GsMTx4 membrane binding

The molecular dynamics modeling predicts that GsMTx4 interacts with membranes in a deep binding mode as shown in Figure 1. It is predicted that this mode of binding may be important to GsMtx4 inhibitory effect on MSCs.

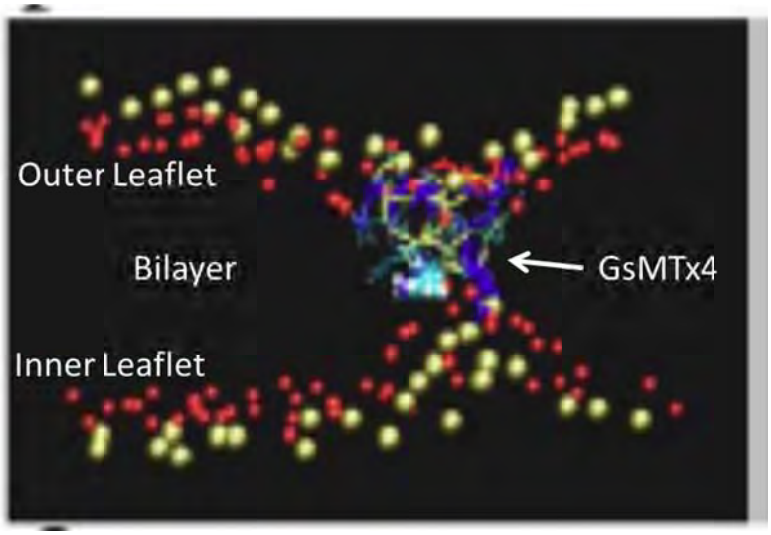

Figure 1 Cartoon model based on molecular dynamics simulations suggests GsMTx4 enters the bilayer in a deep binding mode that produces significant distortion of the membrane. This distortion may underlie GsMTx4 inhibitory effect on MSCs which sense bilayer tension and curvature. Positive charge residues interacting with the negatively charged carbonyl head groups on both the outer and inner leaflets of the bilayer are predicted to stabilize this mode of interaction. Blue groups on

GsMTx4 represent positively charged amino acids and red groups in membrane represent negatively charged carbonyl groups.

In deep binding mode, some of the positively charged residues on GsMTx4 are predicted to interact with the inner leaflet carbonyl groups to stabilize the interaction. These positively charged residues would have a relatively greater impact on the peptide inhabiting this deep state than residues near the outer leaflet, because their interaction with inner leaflet carbonyls are responsible for overcoming the energy barrier of pulling the peptide through the membrane. The lower the energy of the final state, the more likely the peptide will inhabit the deep binding state. This would be manifested in inhibitory potency of the peptide on MSC currents if this state is responsible for blocking the channels. The model predicts that, if the peptide adopts the confirmation in the membrane shown in Figure 1, four of the six lysine residues on GsMTx4 (K8, K20, K25 and K28) would be able to associate with the inner leaflet while the other two (K15 and K22) would not. Calculating the free energies associated with deep binding for the six different K to E mutants shows that the greatest decrease in free energy is associated with the four lysines that can interact with the inner leaflet.

So we synthesized the six different K to E mutants of GsMtx4 to test this hypothesis. We made outside-out patches from Piezo 1 expressing HEK cells since these channels are stretch sensitive and shown to be inhibited by GsMTx4 (Bae et al., 2011). We then perfused the different GsMTx4 mutants onto these patches and measured the rates of inhibition and recovery after washout of Piezo 1 current as shown in Figure 2. We used these measurements to calculate the association and dissociation constants. K25 and K28 showed no block at all and so their kinetics could not be calculated. From the k_a and k_d for the other mutants we calculate the equilibrium dissociation constant (K_D). Our inhibition and recovery data show that, along with K25 and K28, mutants K8E and K20E produce the greatest decrease in affinity (Figure 3). This data is consistent with a model where GsMTx4 inhabits a deep binding mode in an orientation allowing these four lysines to interact with the inner leaflet of the bilayer and thus having a greater contribution to stabilizing this mode of interaction. It also supports the idea that deep binding mode is important for GsMTx4 inhibition of MSCs. The two lysines predicted to be facing the extracellular side had no significant effect on inhibition.

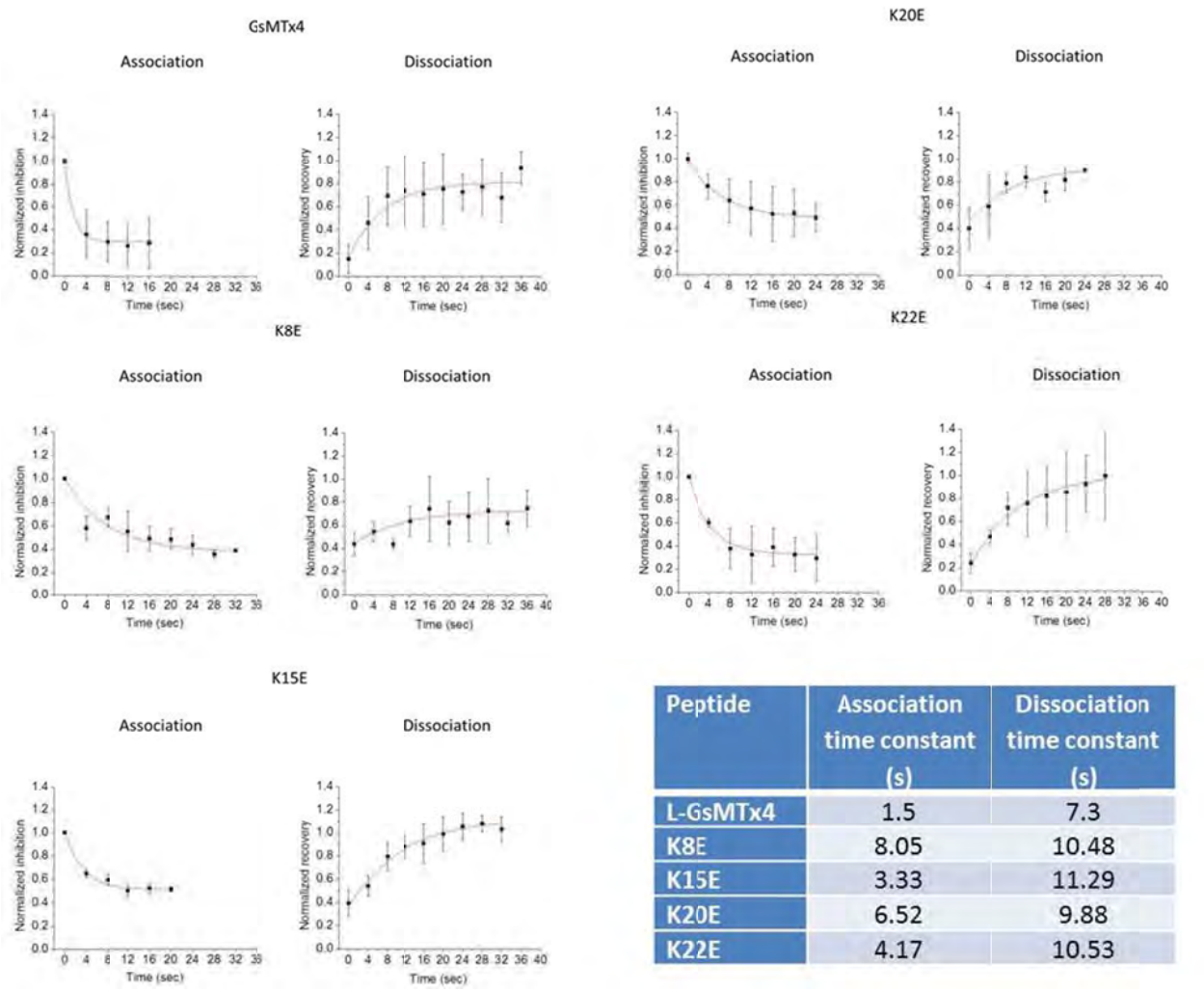

Peptide	Association time constant (s)	Dissociation time constant (s)
L-GsMTx4	1.5	7.3
K8E	8.05	10.48
K15E	3.33	11.29
K20E	6.52	9.88
K22E	4.17	10.53

Figure 2 Shows the rates of MSC current inhibition and recovery after washout for wt GsMTx4 and 4 KtoE mutants applied to outside-out patches. Currents are averaged from 500 ms pressure steps applied to the patches at 4 second intervals. From the inhibition and recovery times we calculated the association and dissociation rate constants in the table.

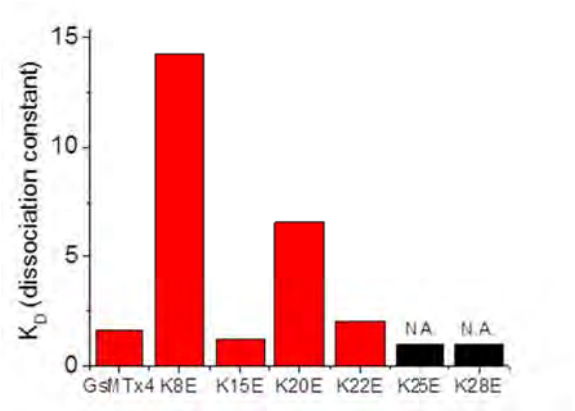

Peptide	K_D
GsMTx4	1.65771
K8E	14.24486
K15E	1.22156
K20E	6.59762
K22E	2.05793
K25E	N.A.
K28E	N.A.

Figure 3 Calculated K_D for wt and K to E mutant GsMTx4 peptides. The reduction in K_Ds for the four lysines predicted to interact with the inner leaflet have the lowest inhibitory effect consistent with a model where deep binding mode is important for inhibition

We will continue these studies by mutating aromatic residues on the hydrophobic face of GsMTx4 to the polar residue threonine. We have shown that a protected Cys-(tbut) can be added to the N-terminus of GsMTx4 with little effect on its activity (see Sept. 14, 2012 update). Our next step is to attach a fluorophore to this free cysteine to determine if GsMTx4 localizes to punctae on the cell surface which would suggest association with membrane domains. If this occurs we will look for colocalization with various channels and scaffolding proteins such as caveolin.

Aim 2) The goals of this aim are to study the effects of inflammatory agents on MSC gating kinetics in both the patch and in whole cell currents from isolated differentiated DRG neurons and from the DRG model cell line F-11. To do this we are incorporating a variety of techniques to mechanically stimulate cells and to measure the channel activity. A sub goal is to identify the MSC protein subunits in DRGs involved in the inflammatory response and to investigate how their gating properties are affected by inflammatory mediators.

Effects of inflammatory agents on patches and whole cell currents from neurons

In the first part of this aim we have made considerable progress toward characterizing the patch currents in DRGs and F-11 cells (Figure 4 and see Dec. 6, 2012 update). However due to the low frequency of the patches with channel activity and the significant variability in the channel response we have focused our testing of inflammatory mediators on the whole cell currents activated by probe indentation of the cell body. There is evidence that a primary component of these currents is produced by the recently discovered MSC called Piezo 2 (Coste et al., 2010; Kim et al., 2012)(see below). After cloning of this channel into the proper expression vector we will continue with the patch analysis when we will be able to produce a more frequent and robust response in the patches from both cell types.

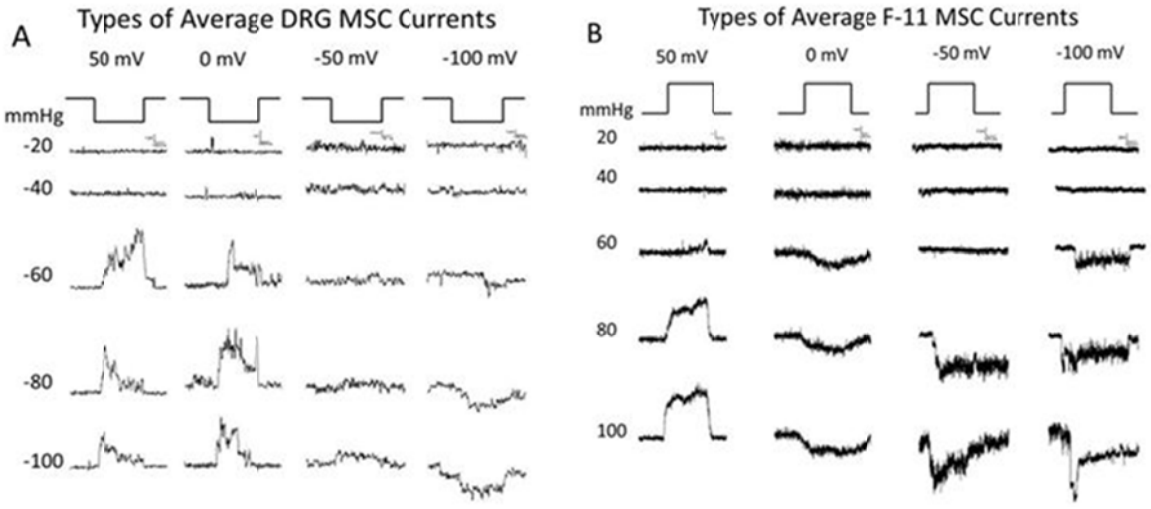

Figure 4 Single channel records of the different MSCs responses observed in small to medium DRGs (A) and F-11 (B) cells. Currents are shown at different voltages for increasing pressure stimuli. The most common MSC activity observed in DRGs

were rapidly inactivating where the inactivation showed pressure sensitivity as observed for the first set of records ranging from -60 to -100 mmHg (A). F-11 cells most typically showed non-inactivating currents as observed in the first row (B). However, a range of inactivation properties were observed for both cell types.

Indentation of DRG neurons elicits a strong inactivating response in most cells (Figure 5) which is a characteristic of Piezo channels. When cells are treated with PGE2 (a prostaglandin family inflammatory mediator) there is a significant increase in MSC current within minutes which then decreases upon washout. The rapid response suggests a direct lipid based response, but we cannot rule out cytoskeletal changes or activation of secondary messengers yet.

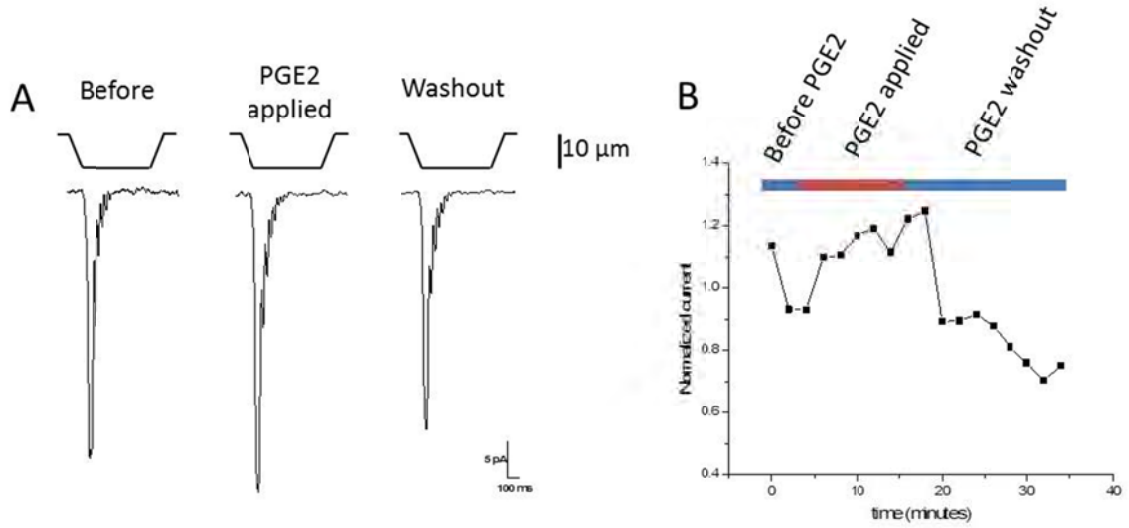

Figure 5 Indentation induced currents in DRG cells increase reversibly when treated with 100 µM PGE2. (A) The indentation stimulus is shown above the actual current records. Notice the current shows a rapid inactivation. This is a property of Piezo channels. (B) The response is rapid (1-2 minutes) as shown in the average peak currents from multiple cells suggesting that PGE2 may act directly on channels rather than through cytoskeletal remodeling or activation of secondary messengers.

Doing the same experiments with 5HT has produced a variable response which is likely related to the heterogeneity in DRG cultures. This heterogeneity has become a significant impediment to understanding the average responses and thus characterizing the response in different neuronal types has become a major effort in our most recent work. We are documenting the size of the cell body and shapes of the neurites as we test indentation and patch currents and will likely see patterns emerge. We are also working on characterizing the different neuronal types in the DRG cultures based on the different response to inflammatory mediators using Ca^{2+} influx and cpstFRET chimeras as measures of the response (see below) and will correlate this data with the current recordings.

Cloning Piezo channels

Since the currents in both the patch and whole cell indentation experiments on DRG neurons show strong inactivation similar to the published Piezo currents, we have embarked on cloning the Piezo 2 gene into the pIRES expression vector. This vector expresses both the gene of interest along with GFP as an indicator of expression. When we received the mouse Piezo 2 clone from Dr. Arden Patapoutian's lab there was an insertion mutation present at the C-terminal end that we were unaware of at first and disrupted expression and cloning into the pIRES vector. We have been working on correcting this mutation and have successfully cloned part of the mouse Piezo 2 gene into the pIRES vector. A small

part of the distal end of the gene needs to be introduced into the vector yet. We are amplifying this region from cDNA synthesized from mRNA derived from DRG neurons. Because the cDNA of these genes exceeds or is near the limit of the cloning capacity of these vectors, cloning them has been challenging. We are also working on cloning mouse Piezo 2 mRNA from the F-11 cell line and have the gene in the cloning vector but are having difficulty transferring the whole gene product to the expression vector. The F-11 clone is interesting because it has several small sequence differences from the DRG clone received from Dr. Patapoutian's lab. It will be interesting to determine if any channel property difference arise due to these sequence changes. We are working on multiple strategies to complete insertion of the both full length clones into pIRES and are close to completing both projects.

We have also recently cloned the human Piezo 2 gene into an expression vector, but have have not been able to produce the full length clone in pIRES. Meanwhile we are cotransfecting human Piezo 2 with a GFP vector to begin studying these channels (se below).

Piezo channels

We co-transfected human Piezo 2 and GFP cDNA into HEK cells and elicited patch currents by applying pressure steps (Figure 6). Human Piezo 2 channel currents show similar rapid inactivation to human and mouse Piezo 1. Piezo 2 are usually multichannel currents as in Figure 6A and are rarely observed as single channels in cell-attached patches as in Figure 6B. This is the first time that Piezo 2 channels have been recorded in the patch as there first description in (Coste et al., 2010) they were only observed in whole cell recordings. We also observed the Piezo 2 currents in outside-out patches and showed they are inhibited by 5 µM GsMTx4 (Figure 6C) as are Piezo 1 currents. Upon completion of cloning the two rodent Peizo 2 clones we will begin expression in DRGs and F-11 cells to determine the effects of inflammatory agents on its activity. In addition we will be able to start testing the different GsMTx4 mutants on Peizo 2 as well as Piezo 1 to look for differences in sensitivity. This will help us understand the peptides interaction with MSCs and possibly identify differences in the domains where these channels are sequestered.

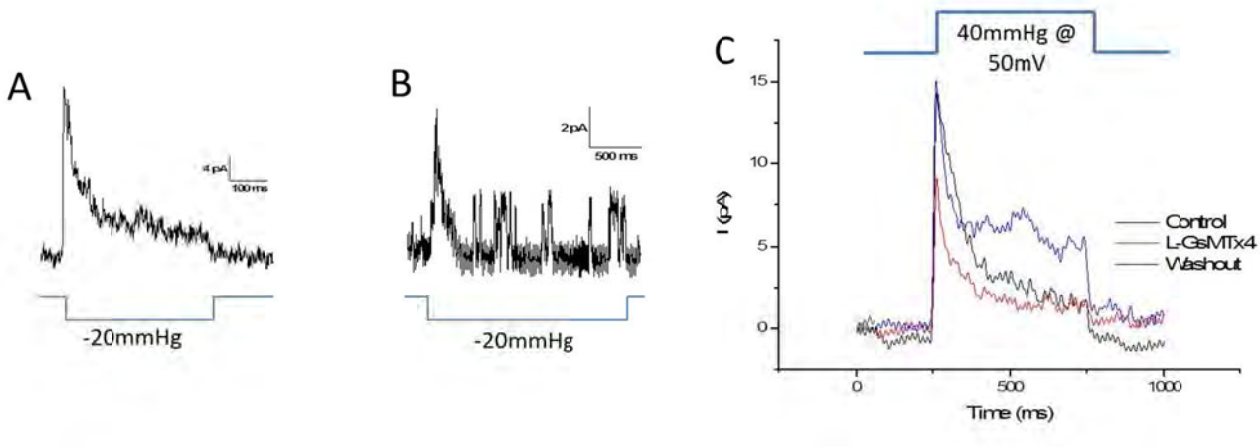

Figure 6 Human Piezo 2 expression in HEK cells produce patch currents similar to Piezo 1. (A) Shows most common form of currents observed in cell attached patches. (B) Shows single channel records in cell attached mode. (C) Average Piezo 2 currents from an outside-out patch before, during and after washout of GsMTx4 shows the channels are sensitive to GsMTx4.

In a recent PNAS publication (Bae et al., 2013) we determined a key region of Piezo proteins involved in the inactivation of these channels. Inactivation is an important property common to most channel types used to control the length of the response. In the disease xerocytosis, hemolytic anemia results from mutations to Piezo 1. Two mutations (M2225R and R2456H) have been identified and we assessed their effect on Piezo 1 function by introducing them into the Piezo 1 gene, expressed them in HEK cells and measured changes to the mechanical response. Whole-cell mechanical currents were evoked using the indentation assay (Figure 7). Both mutants, M2225R and R2456H, had slower inactivation kinetics than wt, while GFP-transfected control cells produced no mechanically activated current (data not shown). Interestingly, a conservative mutation of R to K intended to reverse the loss of inactivation instead slowed inactivation even further.

These results were verified using single channel techniques as well as outside out patches. A unique characteristic of the mutant channels, not seen in the wt, was a pronounced latency to activation observed in the single channel recordings. For hundreds of ms following the application mechanical stimulus there was no change in the current followed by a sudden activation of many channels. We could not simulate this behavior with a Markov model even with many closed states and we postulate that the latency reflects a stress-induced physical rupture of a domain containing the channels.

We have compared this region of the protein with the sequence for hP2 and noted that there is homology between the two proteins. Our results predict that mutations made to this region in hP2 would also slow inactivation. Given that hP2 is located mainly in the dorsal root ganglia such mutations may be involved in chronic pain since cells would be more prone to excitation and nocioceptive response. Since the peptide GsMTx4 blocks these channel even in the mutated state, there is the possibility that the peptide can be used to block channel response.

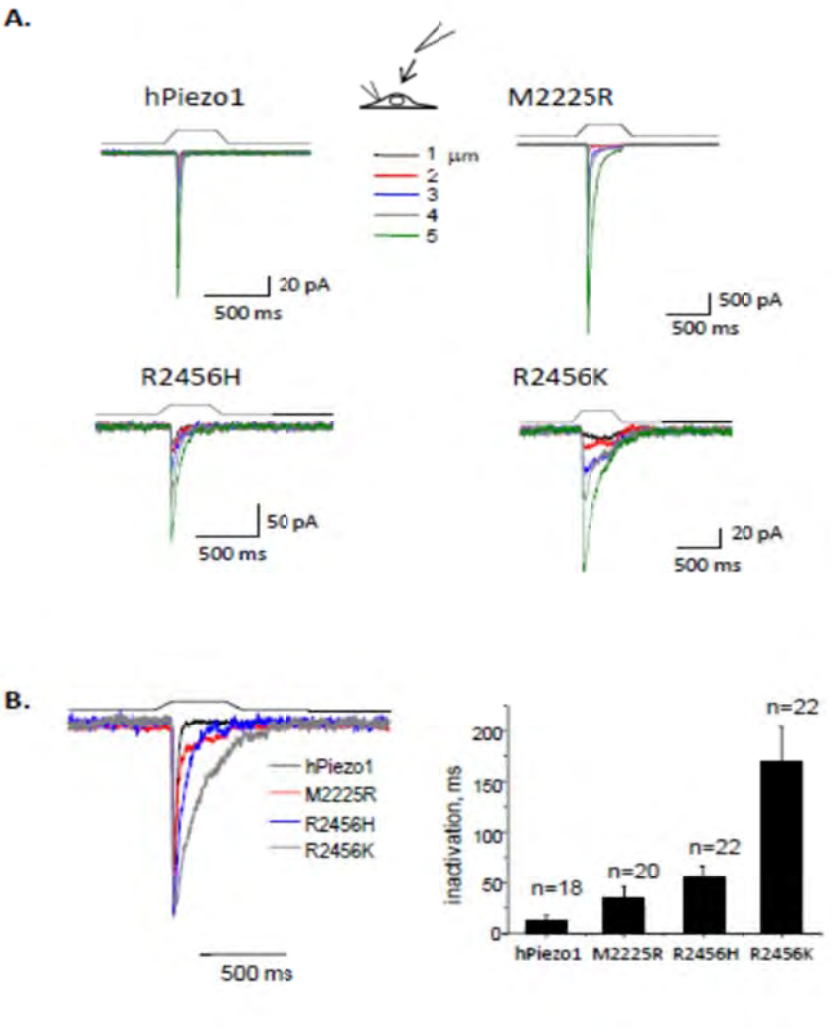

Figure 7 The effect of HX mutations on whole-cell currents. The mutations were introduced at positions 2225 or 2456. HEK293 cells were transfected with ~1 µg of DNA and measured 24-48 hours later. Panel A shows whole-cell currents as a function of depth of the indenting probe. The stimulus waveform is shown above the current trace. Panel B is an average of repeated current traces (right panel) showing the slowing of inactivation for both M2225R and R2456H. These traces have been normalized for kinetic comparison. The conservative mutation that replaced arginine with lysine at position 2456 (R2456K) was intended to measure the effect of residue charge. Despite maintaining charge, the mutation completely removed inactivation suggesting that this site may be part of a hinge domain. The bar graph shows the mean response ± SD.

Aim 3) In this aim we are investigating the stress distribution on different cytoskeletal proteins in DRGs using the FRET based stress reporting probes we have developed. Constitutive stress levels in the cell body and neurites will be measured and changes in stress after treatment with inflammatory agents. We will also induce macroscopic stress in the DRGs with probe pressure in different regions of the cell and monitor the currents and the GsMTx4 sensitive Ca^{2+} influx.

Expression of cpstFRET chimeras in DRGs

DRG neurons are highly resistant to transfection as are most differentiated cell types. Normal transfection methods (Fugene derivatives, Lipofectamine, $CaPO_4$ precipitation) were completely

unsuccessful. We tried different pretreatments with serum conditions which were reported to work on DRGs also without success. We tried constructing adenovirus clones of the different cpstFRET chimeras but the cDNA insert was too large for inclusion in the viral head particle and we obtained very low titers. Finally we have worked out conditions using electroporation that gives us transfection, although with very low efficiency. With the few cells that we obtain we were able to begin assessing the stress on actinin and filamin at rest and after treatment with inflammatory reagents. We are continuing to modify the protocol (cell density, DNA concentration, length of stimulus) to improve efficiency.

A major impediment to assessing MSC activity in DRGs is the variability in the response mechanical stimuli due to the heterogeneity of the cultures. Figure 8 A-D provides a sampling of the cell types which we are working to roughly categorize so that responses can be standardized prior to assessing changes caused by inflammatory agents. The main categorization method is based on cell body shape and diameter and neurite arborization. There are 3 main cell diameters that are roughly categorized as small (10-20 μm), medium (20-30 μm) and large (30-40 μm). These can be subdivided into rounded and flat cell bodies. These categories can be associated with one of the 3 arborization patterns: extended low frequency branching, compact thin fiber high frequency branching, and compact thick fiber high frequency branching.

When filamin and actinin cpstFRET chimeras were expressed in DRGs, different levels of resting stress were observed for these two cytoskeletal adaptors (Figure 8G), with actinin showing the higher resting stress similar to findings in most other cell types we have tested. We then recorded the response of actinin and filamin when treated with inflammatory agents (Figure 8E & F). Actinin has little response to the treatment with 5HT whether in the cell body or in the neurites. In our June 8 progress report we showed that there are differences in response of Actinin based on its location in the neurite. For this report we have only assessed the neurites as a whole. We will need to develop new automated analysis techniques to recognize and monitor certain structures within the neurite since manual analysis time of individual neurite structures would prohibitively long. However, since most of our patching and pressing assays are performed on the cell body we will focus our experiments on this region. This is not detrimental to the studies because we have observed that the cell body actively reacts to inflammatory stimuli as shown in our Dec. 6 progress report where cell blebbing (cytoskeletal remodeling) was coincident with Ca^{2+} influx. When we treated filamin cpstFRET expressing DRGs with 5HT and PGE2 we again observed little or no response in the neurites, but many cell bodies showed significant changes in FRET (Figure 8F). This result shows two things; 1) the cell body does respond mechanically to the inflammatory mediators making electrical recordings and mechanical stimulation of this region relevant and important, and 2) filamin is more sensitive to the inflammation response than actinin suggesting filamin changes in stress may coincide with the changes with MSC activity. This is a different result than what we observed in F-11 cells where none of the cpstFRET chimeras tested (actinin, filamin and spectrin) showed significant sensitivity to 5HT (see Sept. 14, 2012 progress report). As we accumulate more data from indentation currents and FRET changes we will compare the timing of the changes that occur. Now that we are generating more expressing neurons per coverslip these experiments will progress rapidly.

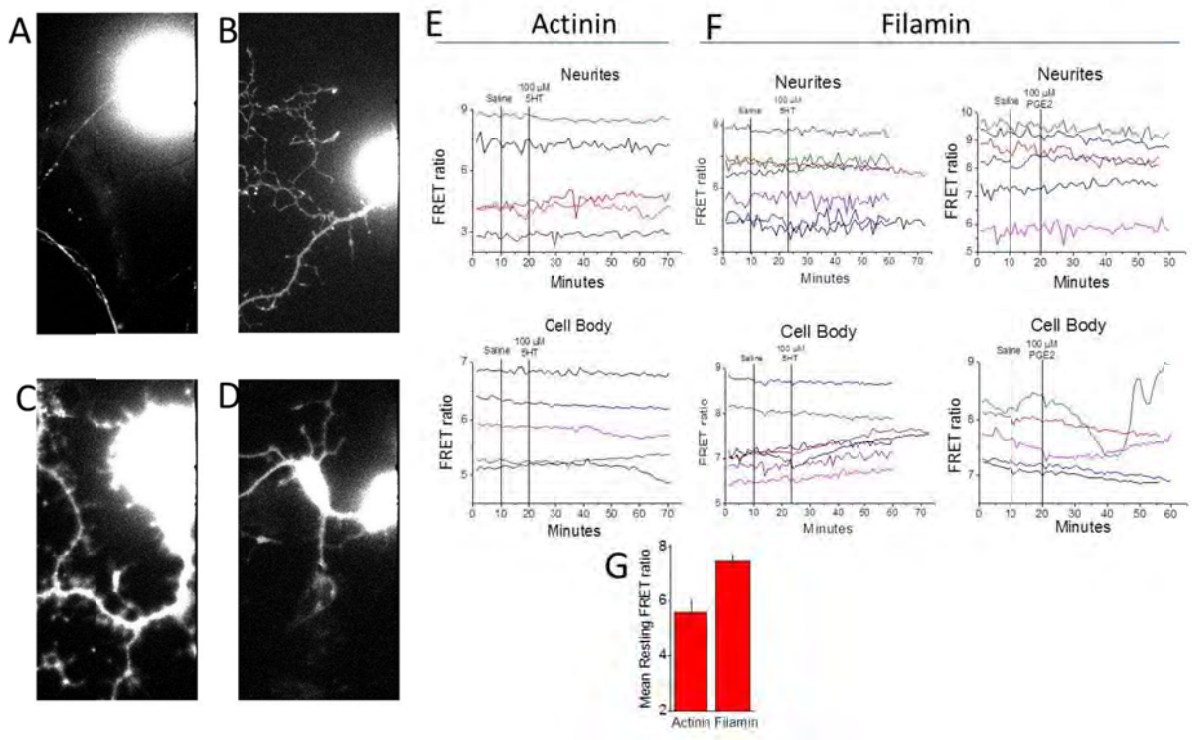

Figure 8 DRG sizes and morphologies, and different cytoskeletal responses to inflammatory agents. The images on the left show the different types of DRGs that we encounter expressing cpstFRET chimeras – (A) Actinin expressing, medium sized cell body and long thin extended neurites and few branch points, (B) Actinin expressing, small cell body with highly branched compact thin neurites, (C) filamin expressing, large flat cell body with thick branching neurites ("ink blot"), (D) filamin expressing, small flat cell body with thick branching neurites ("ink blot"). (A and B) are the most commonly observed types of neurons, but the ink blot type were identified (Dubin et al., 2012) as displaying nociceptive type currents that were sensitive to Piezo2 miRNA. (E) Recordings of the FRET ratio over 70 minutes from Actinin cpstFRET expressing cell bodies and neurites with control saline change alone or the addition of 100 µM 5HT occurring at the times indicated by the line markers. Actinin shows little sensitivity to 5HT. (F) Same recordings as in (E) but with DRGs expressing filamin cpstFRET. In these recordings many cell bodies showed a response to treatment with both 5HT and PGE2. However the neurites again showed little change possibly due to the heterogeneity in the structures all being averaged together. (G) Shows the average resting FRET ratios for actinin and filamin indicating that actinin has a higher resting stress level.

Aim 4) This aim was to determine the potential therapeutic use of GsMTx4 for pain by in-vivo testing in rats. Using the current data on positive charged mutants and the cys-GsMTx4 we are prepared to start developing new analogs of GsMTx4 that have higher affinity and affect different properties of the gating, such as the residual current or inactivation or stronger inhibition of the total current. If any of these are realized prior to the conclusion of the grant we will begin testing them in the rat pain model.

Key Research Accomplishments:

Aim 1)

We have concluded the testing of GsMTx4 lysine mutants and showed that the location of the positively charged residues is important to GsMTx4 binding. The relative influence of the different lysines to binding is consistent with a molecular dynamics model suggesting GsMTx4 enters a deep binding mode that is critical to its function. We are currently preparing this manuscript.

Aim 2)

- We have characterized mechanically activated currents and in DRGs and the F-11 neuronal cell line in both the patches and in whole cell recordings. We have have observed Piezo 2 like currents in both cell types which are related to nocioceptive neuron currents.
- We have decided to focus on the indentation induced whole cell current assay for testing inflammatory agents due to the greater consistency in the response.
- DRGs show a rapid increase in sensitivity to indentation after treatment with PGE2.
- We have cloned the human form of Piezo 2 and are close to completing insertion of two different mouse Piezo 2 clones in the pIRES expression vector.
- We have expressed human Piezo 2 in HEK cells and showed its single channel properties for the first time are rapidly inactivating as reported for whole cell currents in the literature.
- We have shown Piezo 2 patch currents are blocked by GsMTx4.
- We published a report identifying key regions of Piezo 1 channels responsible for controlling channel inactivation. These regions are similar in Piezo 2.

Aim 3)

- We have tested many methods for transfecting DRG cells with cpstFRET chimeras and worked out the best conditions for expression.
- We have shown that DRGs have significant variability in their response to inflammatory mediators based on both the Ca^{2+} influx assay and monitoring FRET changes in cells expressing cpstFRET chimeras.
- We showed that the cell body is a good indicator of cytoskeletal changes and that the stress on filamin changes more in response to inflammatory agents than actinin.

Aim 4)

- Progress on this aim is awaiting new forms of GsMTx4.

Reportable Outcomes:

Publications:

Xerocytosis is caused by mutations that alter the kinetics of the mechanosensitive channel PIEZO1, Chilman Bae, Radhakrishnan Gnanasambandam, Chris Nicolai, Frederick Sachs, and Philip A. Gottlieb, PNAS 2013 110 (12) E1162-E1168; published ahead of print March 4, 2013, **See attached paper.**

Lysine mutagenesis confirms GsMTx4 tarantula peptide inhibits MSCs through a deep binding mode interaction with membranes, Radhakrishnan Gnanasambandam, Frederick Sachs, Kazu Nishizawa, Thomas M. Suchyna, (in preparation for submission to Biophysical Journal).

Conclusions:

We have made considerable progress on all aspects of the first 3 aims. In the first aim we have produced evidence for the method of peptide interaction with the membrane that is crucial for its inhibitory activity. These findings will not only help us in design mutants of GsMTx4 with different properties, but they represent a fundamental difference in the mode of inhibition compared to other related tarantula peptides. The deep binding mode likely underlies GsMTx4s selectivity of action against MSCs. In the second aim we have shown that MSCs currents are responsive to the inflammatory agent PGE2 and that the currents in DRGs have many of the properties associated with the Piezo 2 channel which is blocked by GsMTx4. This is encouraging for continued investigation of GsMTx4 and its derivatives as potential therapeutic agents for chronic pain. We have defined the residues on Piezo 1 channels responsible for controlling inactivation; a crucial function for regulating the response of MSCs to mechanical stimuli. We have cloned and expressed the human form of Piezo 2 and are very close to cloning the rodent form of this channel into the pIRES expression system. This new clone will be crucial to the contimued investigation of the MSCs in pain sensation. We have finally established conditions to express the cpstFRET chimeras in DRGs and this promises to open a whole new field in the investigation of cytoskeletal control of MSCs. From all our previous studies into MSC regulation, cytoskeleton plays one of the most crucial roles in modulating MSC reponse.

References

Bae, C., R. Gnanasambandam, C. Nicolai, F. Sachs, and P.A. Gottlieb. 2013. Xerocytosis is caused by mutations that alter the kinetics of the mechanosensitive channel PIEZO1. *Proc Natl Acad Sci U S A*. 110:E1162-8.

Bae, C., F. Sachs, and P.A. Gottlieb. 2011. The mechanosensitive ion channel Piezo1 is inhibited by the peptide GsMTx4. *Biochemistry*. 50:6295-300.

Coste, B., J. Mathur, M. Schmidt, T.J. Earley, S. Ranade, M.J. Petrus, A.E. Dubin, and A. Patapoutian. 2010. Piezo1 and Piezo2 are essential components of distinct mechanically activated cation channels. *Science*. 330:55-60.

Dubin, A.E., M. Schmidt, J. Mathur, M.J. Petrus, B. Xiao, B. Coste, and A. Patapoutian. 2012. Inflammatory signals enhance piezo2-mediated mechanosensitive currents. *Cell Rep*. 2:511-7.

Kim, S.E., B. Coste, A. Chadha, B. Cook, and A. Patapoutian. 2012. The role of Drosophila Piezo in mechanical nociception. *Nature*. 483:209-12.

Xerocytosis is caused by mutations that alter the kinetics of the mechanosensitive channel PIEZO1

Chilman Bae[a,b], Radhakrishnan Gnanasambandam[a,b], Chris Nicolai, Frederick Sachs[a,b,1], and Philip A. Gottlieb[a,b,1]

[a]Department of Physiology and Biophysics and [b]The Center for Single Molecule Biophysics, State University of New York at Buffalo, Buffalo, NY 14214

Edited by David E. Clapham, Howard Hughes Medical Institute, Children's Hospital Boston, Boston, MA, and approved February 5, 2013 (received for review November 13, 2012)

Familial xerocytosis (HX) in humans is an autosomal disease that causes dehydration of red blood cells resulting in hemolytic anemia which has been traced to two individual mutations in the mechanosensitive ion channel, PIEZO1. Each mutation alters channel kinetics in ways that can explain the clinical presentation. Both mutations slowed inactivation and introduced a pronounced latency for activation. A conservative substitution of lysine for arginine (R2456K) eliminated inactivation and also slowed deactivation, indicating that this mutant's loss of charge is not responsible for HX. Fitting the current vs. pressure data to Boltzmann distributions showed that the half-activation pressure, $P_{1/2}$, for M2225R was similar to that of WT, whereas mutations at position 2456 were left shifted. The absolute stress sensitivity was calibrated by cotransfection and comparison with MscL, a well-characterized mechanosensitive channel from bacteria that is driven by bilayer tension. The slope sensitivity of WT and mutant human PIEZO1 (hPIEZO1) was similar to that of MscL implying that the in-plane area increased markedly, by ~6–20 nm^2 during opening. In addition to the behavior of individual channels, groups of hPIEZO1 channels could undergo simultaneous changes in kinetics including a loss of inactivation and a long (~200 ms), silent latency for activation. These observations suggest that hPIEZO1 exists in spatial domains whose global properties can modify channel gating. The mutations that create HX affect cation fluxes in two ways: slow inactivation increases the cation flux, and the latency decreases it. These data provide a direct link between pathology and mechanosensitive channel dysfunction in nonsensory cells.

mechanical channels | PIEZO1 mutations | channel domains

Hereditary xerocytosis (HX) is an autosomal dominant disease characterized by dehydrated red blood cells (RBCs) and mild-to-moderate hemolytic anemia. Two familial HX mutations were identified recently in the gene encoding hPIEZO1, a mechanosensitive ion channel (MSC) (1).

Mouse PIEZO1 (mPIEZO1) cloned from Neuro2A cells contains ~2,500 amino acids predicted to have 24–36 transmembrane domains. Using crosslinking and photobleaching techniques, PIEZO1 was shown to assemble as a homotetramer (2, 3) with no other cofactors. Currently it is not known whether the pore is central to the tetramer (intermolecular) or whether each subunit conducts (intramolecular). mPIEZO1 is a cation-selective channel with a reversal potential near 0 mV. The conductance is ~70 pS and is reduced to 35 pS by increasing extracellular Mg^{+2} (3, 4). mPIEZO1, like other cationic MSCs, is inhibited by the peptide GsMTx4 (5) and nonspecifically by ruthenium red (2). Heterologous expression in HEK293 cells is efficient, and mechanical currents can be evoked in whole-cell mode or patches. In cell-attached patches at hyperpolarized potentials, mPIEZO1 activates with ~30 mmHg of pipette suction and inactivates within ~30 ms, a rate that slows with depolarization (2–4).

To explore the biophysical properties of human PIEZO1 (hPIEZO1) that produce HX, we cloned it from HEK293 cells and then duplicated the mutations identified with HX. The mutants had slower inactivation and developed a long latency for activation. We also observed that groups of channels could change kinetics together, implying that they normally exist in confining domains that can fracture with the applied force. We showed by coexpressing MscL from bacteria with hPIEZO1 and its mutants that both PIEZO1 and the mutants have similar dimensional changes during opening (6, 7). The half-maximal activation pressure ($P_{1/2}$) for two mutants was shifted to lower pressures, making them more sensitive in absolute terms. The data suggest that mutant hPIEZO1s cause symptoms by excess cation influx (8) from slow inactivation or by delayed activation resulting from increased latency.

Results

To understand the biophysical consequences of the HX mutations, we first cloned hPIEZO1 from HEK293 cells and then introduced the HX mutations at positions 2225 and 2456 (Fig. 1*A*). hPIEZO1 is 88% homologous to mPIEZO1. The HX mutation of M2225 is thought to reside on the extracellular side and R2456 on the intracellular side of the membrane (the full protein sequence is shown in Fig. S1). We characterized hPIEZO1's electrophysiology by transfection into HEK293 cells. In cell-attached patches, hPIEZO1 had an open time of ~40 ms when fit to a three-state linear model, shut-open-inactivated, with pressure sensitivity needed only in the shut-to-open rate constant (Fig. 1*B*). Cell-attached patches show little endogenous activity (5). Like mPIEZO1, inactivation slowed with depolarization (Fig. 1*C*), and activation was inhibited by GsMTx4 (Fig. 1*D*).

We evoked whole-cell mechanical currents by indenting the cells with a glass probe (2, 4, 9) (Fig. 2*A*). Both mutants, M2225R and R2456H, had slower inactivation kinetics than WT (Fig. 2), whereas GFP-transfected control cells produced no mechanically

Significance

Familial xerocytosis in humans, which causes dehydration of red blood cells and hemolytic anemia, was traced to mutations in the mechanosensitive ion channel, PIEZO1. The mutations slowed inactivation and introduced a pronounced latency for activation. Loss of inactivation and increased latency for activation could modify groups of channels simultaneously, suggesting that they exist in common spatial domains. The hereditary xerocytosis mutants affect red cell cation fluxes: slow inactivation increases them, and increased latency decreases them. These data provide a direct link between pathology and mechanosensitive channel dysfunction in nonsensory cells.

Author contributions: F.S. and P.A.G. designed research; C.B., R.G., and P.A.G. performed research; C.N., F.S., and P.A.G. analyzed data; and F.S. and P.A.G. wrote the paper.

The authors declare no conflict of interest.

This article is a PNAS Direct Submission.

Freely available online through the PNAS open access option.

Data deposition: The sequence for human PIEZO1 has been deposited in the National Center for Biotechnology Reference Sequence data bank (accession number KC602455).

[1]To whom correspondence may be addressed. E-mail: sachs@buffalo.edu or philgott@buffalo.edu.

This article contains supporting information online at www.pnas.org/lookup/suppl/doi:10.1073/pnas.1219777110/-/DCSupplemental.

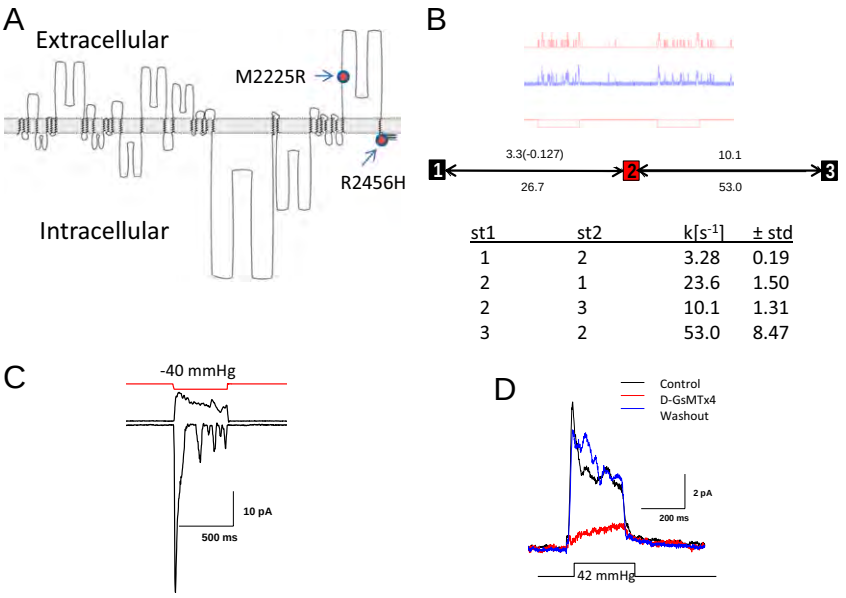

Fig. 1. Characterization of cloned hPIEZO1. (*A*) A diagram showing the putative transmembrane domains of hPiezo1 and intracellular and extracellular regions. The HX mutation sites are shown where M2455R is thought to be extracellular and H2456 is intracellular. (*B*) Kinetic data and a fitted model for hPIEZO1 with three states (closed-open-inactivated). The theoretical fit to the model shown in red provided the kinetic rate constants shown in the table. The pressure dependence is shown in parenthesis. (*C*) Voltage-dependent inactivation. At depolarized voltages (+40 mV) there is slow inactivation, and at hyperpolarized voltages (−110 mV) there is rapid inactivation. (*D*) hPIEZO1 is inhibited by the D enantiomer of GsMTx4 (2 μM, +50 mV holding potential).

activated current (Fig. S2*A*). These results illustrate both transfection specificity and the "mechanoprotection" of the endogenous channels. We explored the generality of whole-cell mechanoprotection by comparing these results with cells transfected with DNA for TREK-1, a K^+ selective MSC (10, 11). This transfection produced small whole-cell currents, but patches from the same cells had large currents (Fig. S2*B*) so that in the whole-cell configuration TREK-1 also was protected from stress, as we assume MSCs are in situ.

Single-channel recordings also showed kinetic differences between the mutants and WT (Fig. 3). A unique characteristic of the mutant channels, not seen in the WT, was a pronounced latency to activation (Fig. 3, compare *Insets*). For hundreds of milliseconds following the application of suction, there was no change in the current, followed by a sudden activation of many channels. We could not simulate this behavior with a Markov model even with many closed states, and we postulate that the latency reflects a stress-induced physical rupture of a domain containing the channels (see below).

We measured the dose–response curve (current vs. pressure fit to a Boltzmann distribution) for hPIEZO1 and the mutant channels. R2456H and R2456K exhibited a leftward shift of 13 and 8 mmHg, respectively, in the $P_{1/2}$, but M2225R was similar to the WT channel (Fig. 4*A*). The leftward shift may represent decreased stress within the resting channel protein or differences in local stress felt within a domain. In the case of TREK-1, it is known that transfection alone causes massive change to the cytoskeleton (12). In contrast to the changes we observed in $P_{1/2}$, the slope sensitivity α (the maximum slope of Popen vs. pressure) was similar for WT and the hPIEZO1 mutants (7–8 $mmHg^{-1}$). The constant α is proportional to the dimensional change between the closed and open conformations and suggests that the mutations did not affect the domains responsible for activation (13).

To provide an absolute measure of α, we cotransfected cells with MscL (14), a bacterial MSC known to be activated by bilayer tension and previously calibrated (7, 15, 16). The plots of peak current vs. pressure curves were fit to the sum of two Boltzmanns, one for the channel under test and one for MscL (Fig. 5). We performed this operation for hPIEZO1 (Fig. 5), two PIEZO1 mutants (Fig. S3), and TREK-1 (Fig. 5). The ratio of α for hPIEZO1 to MscL was 1.15 ± 0.14, $n = 5$, equivalent to a change of ~6–20 nm^2 in the in-plane area (6, 7) (assuming that both populations felt the same tension). The α was similar in the two mutant hPIEZO1 channels. However, for TREK-1, the α ratio was only 0.54 implying that this channel had a smaller dimensional change or that the local tension was about half that of

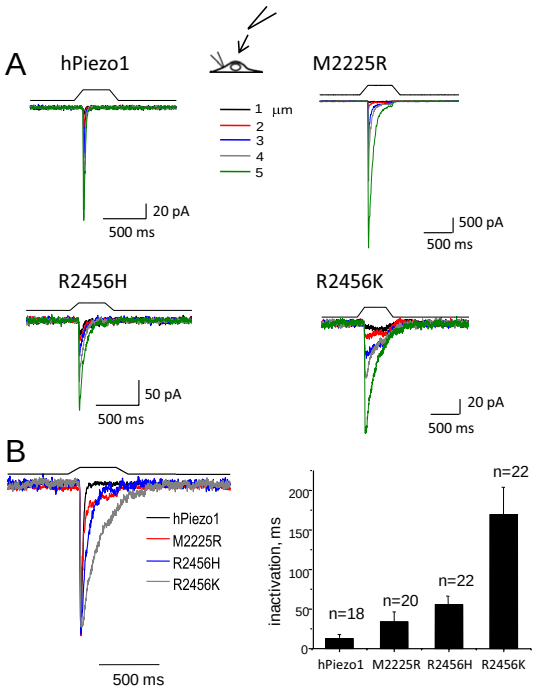

Fig. 2. The effect of HX mutations on whole-cell currents. The mutations were introduced at positions 2225 or 2456 (see sequence in Fig. S1). HEK293 cells were transfected with ~1 μg of DNA and measured 24–48 h later. (*A*) Whole-cell currents as a function of depth of the indenting probe. The stimulus waveform is shown above the current trace. (*B*) (*Left*) Average of repeated current traces showing the slowing of inactivation for both M2225R and R2456H. These traces have been normalized for kinetic comparison. The conservative mutation that replaced arginine with lysine at position 2456 (R2456K) was intended to measure the effect of residue charge. Despite maintaining charge, the mutation completely removed inactivation, suggesting that this site may be part of a hinge domain. (*Right*) The bar graph shows the mean response ± SD.

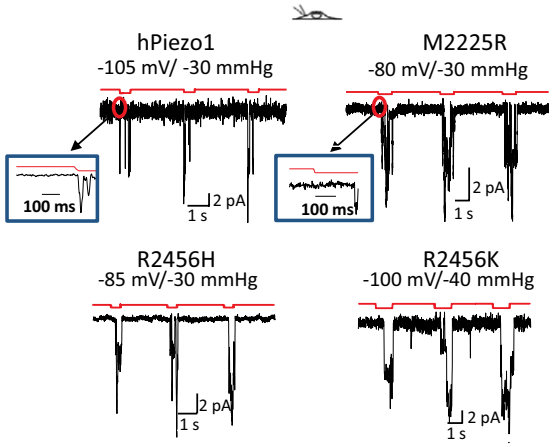

Fig. 3. hPIEZO1 mutations slow inactivation in cell-attached patches at single-channel resolution. M2225H and R2456H slow inactivation, and R24565 removes inactivation. (*Insets*) All three mutants introduced a profound latency for activation not seen in the WT.

the bilayer containing MscL, i.e., they resided in a different mechanical domain(s). These measurements provide an absolute measure of energetics of eukaryotic MSC gating.

Why did the mutations slow inactivation? R2456H resides near the cytoplasmic end of the C-terminal transmembrane span (Fig. 1*A*) and might be in the membrane electric field. To investigate whether the loss of charge associated with this mutation might account for the loss of inactivation, we substituted lysine for the arginine found in the WT. The resulting R2456K mutation did not inactivate and also exhibited slow deactivation (channel closing after removal of the stimulus) (Fig. 2 *A* and *B*). Residue charge did not appear to be involved. Interestingly, it is known that arginine can be modified posttranslationally, and the data from R2456K suggest such a biological change could shift the channel kinetics from phasic to tonic (17–19).

We observed some kinetic differences between cell-attached and excised patches suggesting that the cytoskeleton contributes to stress at the channel (20). In cell-attached mode, M2225R inactivated more slowly than in outside-out (O/O) patches (compare Fig. 6 and Fig. S4). The cell-attached response for a multichannel patch illustrating the loss of inactivation for mutant channels is shown in Fig. S4. Fig. 6 *A* and *B* shows data from O/O patches in which inactivation was restored almost completely in M2225R and was restored partially in R2456H. However, differences in the peak/steady-state current ratios remained, showing that the substitutions were not functionally identical. Fig. 6*B* shows a normalized average response, illustrating that the ratio of peak to steady-state current (an approximate assay for the relative rates of inactivation and recovery) is greater for mutants than for WT. We observed some small differences in activation kinetics between cell-attached and excised patches, but hPIEZO1 inactivated in both patch modes, and R2456K did not inactivate in either one (Fig. 6 *A* and *B*). GsMTx4 inhibited the WT and mutant channels in O/O patches (Fig. 7). Because the non-inactivating mutant R2456K was inhibited by GsMTx4, the peptide's ability to inhibit channel activity does not appear to involve the protein region needed for hPEIZO1 inactivation.

Both HX mutations were near the C terminal of hPIEZO1, so we examined the functionality of the whole region by removing it with a stop codon at position 2218 (G2218Stop). Fig. 8 shows that the truncation mutant behaved like R2456K, exhibiting a long latency, slowed or complete loss of inactivation, and very slow deactivation. Because the activation kinetics, other than latency, were largely unaffected, we conclude that the C-terminal region functions as an independent unit responsible for channel closure by inactivation or deactivation and that residue R2456 is a key locus in that region.

Discussion

We have characterized hPIEZO1 in an effort to understand its involvement in xerocytosis (1). The single point mutations slowed inactivation and introduced a long latency followed by activation of groups of channels (Fig. 8*B*). Might these changes lead to the symptoms of HX? One possibility is that they alter the mechanical sensitivity of the channel and thus change the flux of ions that accompanies mechanical stress, particularly as the RBC pass through capillaries. The relationship between cation leakage and hemolytic anemia has been observed for band 3 protein mutations (8). Although these pathways are different, band3 and PIEZO1 mutations may produce hemolytic anemia by the same mechanism.

An important feature of PIEZO1 that may contribute to the clinical presentation is its ability to pass calcium. The net cation flux through hPIEZO1 channels depends on the open time. All the mutations we tested had slower inactivation rates. R2456H had a leftward shift in activation so that it turned on at a lower stress, but M2555R did not. The slowing of the inactivation may be more important than the channel sensitivity to stress. A second, non-

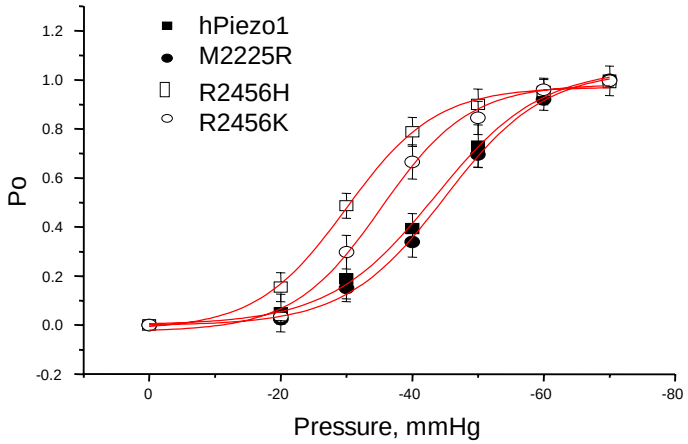

	$P_{1/2}$ (mmHg)	α (mmHg^{-1})	
hPiezo1	-43 ± 0.7	8.1 ± 0.7	n = 10
M2225R	-45 ± 0.6	7.6 ± 0.6	n = 6
R2456H	-30 ± 0.6	6.8 ± 0.4	n =11
R2456K	-35 ± 1.1	6.8 ± 0. 9	n = 7

Fig. 4. Comparison of mechanical sensitivities via peak current vs. suction and fit to a Boltzmann distribution. The mean values ± SD for $P_{1/2}$ and α are shown in the table. The α is approximately the same for the four channels, indicating they have a similar dimensional change between closed and open orientations. Mutations at position 2456 shifted $P_{1/2}$ but the mutation at 2225 did not.

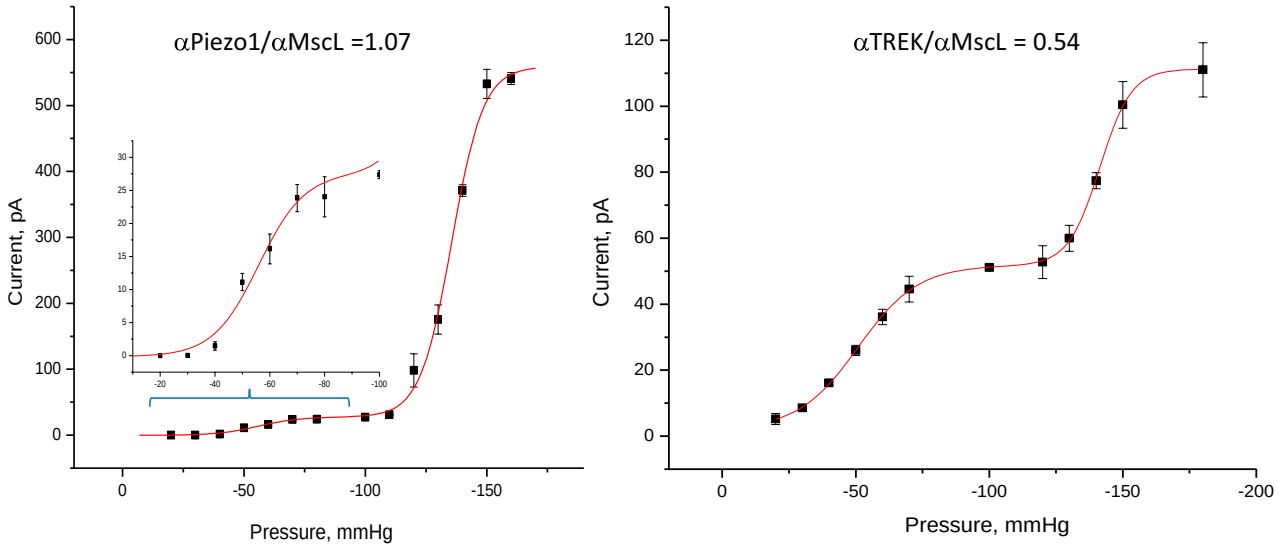

Fig. 5. Comparison of the bacterial channel MscL with Piezo1 or TREK using cotransfection. (*Left*) Current vs. suction for hPIEZO1 and MscL in the same patch. (*Inset*) An expanded view of the hPIEZO1 response curve. (*Right*) The same measurement but using TREK-1. In contrast to hPIEZO1, TREK-1 had a lower ratio of $\alpha_{\text{channel/MscL}}$ indicating either that TREK-1 has smaller dimensional changes or that the local tension around TREK-1 is smaller, as might occur if TREK-1 were in a different domain from PIEZO1.

exclusive possibility is that because of the latency, mutant channels do not activate when needed during capillary transit.

Hydrostatic pressure has been shown to change RBC shape, membrane composition and volume, and to alter the blood flow in small vessels. An influx of Ca^{2+} might alter the stiffness of RBCs (21). The short open-channel lifetime of WT hPIEZO1 restricts significant ion fluxes to the immediate vicinity of the channel, and it is unclear whether such localization is significant.

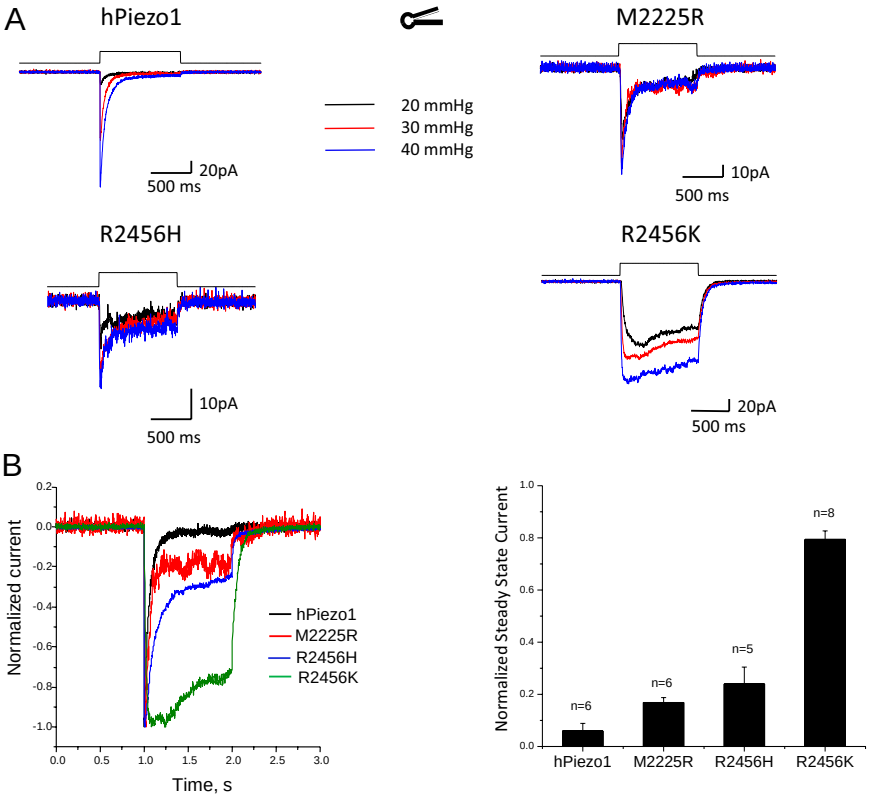

Fig. 6. Response of O/O patches. (*A*) The difference between WT and mutants. M2225R and R2456H have partially restored inactivation; R2456H remains slow; R2456K does not inactivate at all. (*B*) The traces normalized for kinetic comparison. The ratio of peak to steady-state current (bar graph with SD) illustrates that, even with the partial restoration of inactivation, M2225R and R2456H transfer more permeant charge than WT during an opening because of the longer open time. Deactivation (closure upon release of stress) was fast in patches from WT but was slow in mutants.

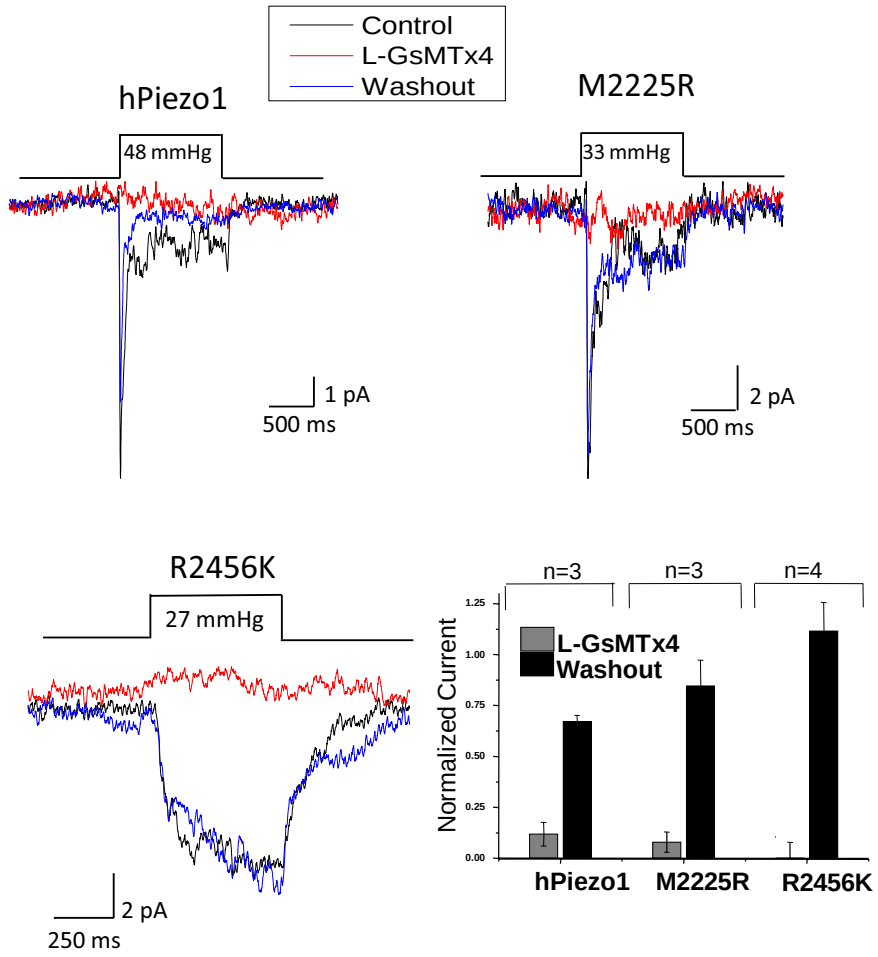

Fig. 7. The peptide L-GsMTx4 (10 μM) reversibly inhibits mutant hPIEZO1 channels in O/O patches from cells transfected with the indicated channels. The bar graph shows the average ± SEM from the indicated number of patches. Note that R2456K did not inactivate but was inhibited, implying that the peptide does not act upon the inactivation domain.

Thus, HX mutations might cause pathology either by too little or too much activation.

The experiments presented in this paper provide molecular details of hPIEZO1 function. Our measurements of α indicate that the dimensional changes associated with opening are similar to those reported for MscL, equivalent to 6–20 nm^2 of in-plane area or an ∼1-nm change in mean radius for a 10-nm diameter channel. If the dimensional changes associated with gating were not global but instead were movements of smaller regions, then there must be a proportionately larger movement to generate the equivalent free energy described by the Boltzmann curves. For the 2D model most commonly used for MSC gating, the free energy available for gating is TΔA where T is bilayer tension and ΔA is the change of area between the closed and open states. These dimensional constraints must be met for any molecular model of hPIEZO1 gating. Because MscL is known to be gated by bilayer tension, we might suppose the same is true for hPIEZO1. If, however, hPIEZO1 were gated by cytoskeleton stress in parallel with the bilayer, the stress on the channel will be decreased because the mean tension is shared. In this case the dimensional changes of hPIEZO1 would have to be larger than MscL to explain the comparable sensitivity. This particular constraint of the dimensional changes does not apply to all MSCs. TREK-1 is half as sensitive as hPIEZO1.

We were surprised that hPIEZO1 appeared to be in discrete physical domains separated from the common bilayer. Channel openings of multiple channels appeared suddenly following a long latency. The channels also often exhibited a collective loss of inactivation (figure 2 in ref. 4 and Fig. 8). As expected for the random sampling of the cell surface by the patch pipette, we occasionally did observe some patches that appeared to have sev-

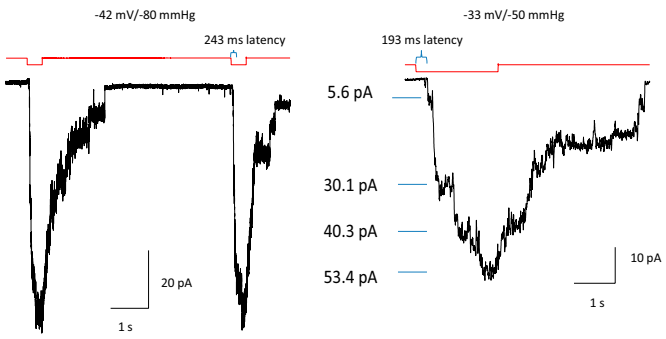

Fig. 8. Removal of the C terminus with a stop codon at position 2218 of hPIEZO1 leads to a non-inactivating form of the channel with pronounced latency, loss of inactivation, and extremely slow deactivation. The slow deactivation might represent the rate for mutant monomers to reassociate. *A* and *B* show the currents from many channels in cell-attached patches, and *B* shows the loss of inactivation in an expanded view. The unitary conductance at −33mV was 73 pS (0.5 mM Mg^{2+} in pipette).

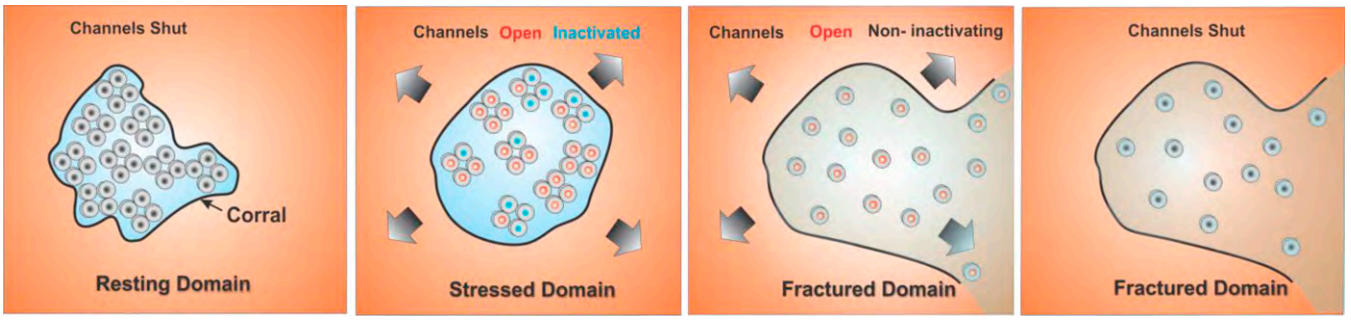

Fig. 9. Cartoon model of how domains might affect channel behavior. We arbitrarily modeled the domain as a cytoskeletal corral. The panel at the far left shows closed WT channels (black) in a domain with a flexible boundary that can transmit external stress without delay. In this domain the channels exist as tetramers. The second panel from the left shows the expansion of the flexible boundary with external tension causing channels to open (red) and to inactivate (blue). The panel third from the left shows what happens when high forces rupture the domain boundary. The channels diffuse outward into the bulk bilayer where the tension is sufficient to activate them, but the tetramers can dissociate. We postulate that inactivation requires channel–channel interactions so the diffusing channels do not inactivate quickly. The right panel shows deactivation in a ruptured domain after tension is removed. In this model, HX mutations would decrease the interchannel-binding energy, allowing easier dissociation. Although the cartoon shows the domain as a corral, the domain may be a lipid phase, caveolae, cytoskeletal structures, or even channel aggregates.

eral domains. In contrast to the mutants, WT hPIEZO1 channels activated without a measurable latency, so the domains of normal resting cells must be able to transmit the applied stimulus coming from the bilayer to the domain interior rapidly without spending time to reform the domain boundary. The collective loss of inactivation and introduction of latency has been observed previously with endogenous MSCs (4, 22). Extreme latencies (with durations in minutes) have been observed for whole-cell mechanically activated currents from heart cells (23). This transition between phasic and tonic kinetics probably represents global changes in the mechanical properties of the domains. However, with high and/or repeated stress the domain boundary can rupture, making the local tension closer to that of the mean bilayer. The modulation of ion channels by lipid microdomains has been described for other channels (24), and the clustering of channels has been noted for many channels such as in the endplate (25).

To simplify the discussion of how domain properties can alter channel kinetics, we made the cartoon model shown in Fig. 9. In this model, the resting domain boundary is folded so there is little line tension, and the external stress is transmitted rapidly to the interior, causing the channels to open and inactivate (second panel from the left). With excessive simulation, the domain ruptures allowing channels to diffuse into the external bilayer (third panel from the left). This diffusion might allow hPIEZO1 tetramers to dissociate, and, if we postulate that inactivation requires interchannel interactions, this dissociation would account for the observed collective loss of inactivation. The forces required for domain rupture are unknown but clearly are less than the lytic limit of the bilayer because the patch remained intact. The actual domains might be cytoskeletal lattices, caveolae, rafts, or other structures, and high-resolution imaging of labeled channels may permit the domains to be visualized (20).

As for the physiological utility of hPIEZO1 in the circulation, the role of hPIEZO1 can be acutely tested in animals using the specific inhibitor GsMTx4 (Fig. 7) (5, 26). A transgenic mouse in which the WT channel has been replaced with the non-inactivating mutant R2456K would make a very interesting test system. hPIEZO1 is one member of the larger PIEZO family (2, 3), and the two HX sites analyzed in this study are conserved in Piezo2 (Fig. 10). Piezo2 is highly expressed in dorsal root ganglia neurons, where its function has been associated with nociception (27). If that channel behaves like hPIEZO1, a transgenic mouse with the same mutations might create a model for chronic pain. Xerocytosis provides an example of how the altered biophysical properties of MSCs can create pathology and illuminates the potential role of these channels in nonsensory tissues.

```
                2225
                 |
hP1    LGGYEPLFTMSAQQPSIPFTA
hP2    LGGYQPIFTMSAQQSQLKIMD

                2456
                 |
hP1   SIVLVIGKFVRGFFSEISHSIMFEEL
hP2   SVVLVIGKFVREFFSGISHSIMFEEL
```

Fig. 10. Sequence comparison between human Piezo1 and Piezo2. The amino acids in Piezo1 involved in xerocytosis also are found in Piezo2. This homology suggests that mutations at these sites in Piezo2 lead to a loss or slowing of inactivation and potential increase in nociception.

Experimental Procedures

Electrophysiology. The bath solution contained (in mM) 145 NaCl, 5 KCl, 3 $MgCl_2$, 1 $CaCl_2$, 10 Hepes (pH 7.3, adjusted with NaOH). The pipette solution contained (in mM) 150 KCl, 0.5 $MgCl_2$, 0.25 EGTA, 10 Hepes (pH 7.3), or, alternatively 150 CsCl, 1 $MgCl_2$, 1 $CaCl_2$, 5 EGTA, 10 Hepes (pH 7.3). Patch pipettes had resistances of 2–5 MΩ. For studies of TREK-1, CsCl was replaced with KCl. The mechanical stimulus for patches was suction applied with a high-speed pressure clamp (HSFC-1; ALA Scientific Instruments) and controlled by QuBIO software (www.qub.buffalo.edu). HEK293 cells were transfected with 250 ng cDNA using Fugene (Roche Diagnostic) and were tested 24–48 h later. GsMTx4 was synthesized, folded, and purified as previously described (26, 28) and was applied to cells through an ALA perfusion system controlled by QuBIO (www.qub.buffalo.edu). All experiments were done at room temperature.

Whole-cell and patch-clamp experiments were performed using an Axopatch 200B amplifier (Axon Instruments) controlled by QuBIO, sampled at 10 kHz, and filtered at 2 kHz. The dose–response data for two different types of channels in a single patch were fit using the sum of two Boltzmann equations, one for each type of channel:

$$I = A + Im1^{*}\left[1 - \frac{1}{\left(1 + e^{\left(\frac{P1-P}{a1}\right)}\right)}\right] + Im2^{*}\left[1 - \frac{1}{\left(1 + e^{\left(\frac{P2-P}{a2}\right)}\right)}\right],$$

where *Imi* is the maximum available current for each channel type *i*, P_i is the pressure at half activation, α_i is the slope sensitivity, and *A* is an instrumental offset. Whole-cell mechanical stimulation used indentation with a fire-polished

glass pipette (tip diameter 2–4 μm) positioned at an angle of 45° to the coverslip. A computer-controlled micromanipulator (MP-285; Sutter Instruments Co.) with LabVIEW software provided coarse positioning of the probe to ∼30 μm from the cell. From there, a further rapid downward trapezoidal waveform of indentation was driven by a piezoelectric stage (P-280.20 XYZ NanoPositioners; Physik Instrumente). We define the mechanical threshold as the depth at which the probe visibly deformed the cell. The probe velocity was 0.56 μm/ms during the upward and downward movements, and the steady indentation was held constant for 400 ms. The stimulus was repeated with 0.5-μm increments every 6 s. The holding potential generally was −60 mV.

Molecular Cloning of HEK hPIEZO1. Total RNA was extracted from HEK293 cells using Quick-RNA MicroPrep (Zymo Research) and was converted to cDNA using the SuperScript III First Strand Synthesis System (Invitrogen). The hPIEZO1 gene was first amplified for 30 cycles using primers 5′-atggagccgcacgtgctcgg-3′ and 5′-ctactccttctcacgagtcc-3′ (designed from NM_001142864). A second round of amplification for 30 cycles used primers with 5′ linkers containing the Nt BbvCI sequence 5′-tcagcaagggctgagg-3′ and 5′-tcagcggaagctgagg-3′. The vector internal ribosome entry site 2 (IRES2)-EGFP was modified to include NtBbvCI sites according to the ligation-independent cloning method using nicking DNA endonuclease (29). Both the hPIEZO1 PCR product and the modified IRES2-EGFP were cut with NtBbvCI in one tube. After 8 h, the enzymes were deactivated by heating to 80 °C for 30 min and then were allowed to cool to room temperature. The DNA was transformed into Dh5Alpha cells (Invitrogen). The amplified DNA sequence of the WT hPIEZO1 cDNA was validated to ensure absence of unwanted mutations introduced by PCR amplification.

Mutagenesis of hPIEZO1. HEK-293 hPIEZO1 mutants M2225R, R2456H, and R2456K were made using the QuikChange XL site-mutagenesis kit (Agilent Technologies) according to the manufacturer's specifications. Primers used were M2225R forward, agccgctgttcaccaggagcgcccagcag; M2225R reverse, ggctgctgggcgctcctggtgaacagcgg; R2456H forward, tcggcaagttcgtgcacggattcttcagc; R2456H reverse, tctcgctaagaatccgtgcacgaacttgc; R2456K forward, tcggcaagttcgtgaagggattcttcagcgagatc; R2456K reverse, ctcgctgaagaatcccttcacgaacttgccgatgacc; G2218Stop forward, caccctgaagctgggctaatatgagccgctgttcacc; and G2218Stop reverse, ggtggacagcggctcatattagcccagcttcagggtg.

ACKNOWLEDGMENTS. We thank Dr. Steve Besch for help in the Boltzmann analysis, Joanne Pazik and Lynn Zeigler for expert technical assistance on the molecular biology, Julia Doerner from David Clapham's laboratory for sharing the eukaryotic vector for expression of the MscL channel, and Drs. Sidney Simon and Seth Alper for extensive editing. This work was supported by the National Institutes of Health, the Department of Defense, and the Children's Guild of Buffalo.

1. Zarychanski Y, et al. (2012) Mutations in the mechanotransduction protein PIEZO1 are associated with hereditary xerocytosis. *Blood* 120(9):1908–1915.
2. Coste B, et al. (2010) Piezo1 and Piezo2 are essential components of distinct mechanically activated cation channels. *Science* 330(6000):55–60.
3. Coste B, et al. (2012) Piezo proteins are pore-forming subunits of mechanically activated channels. *Nature* 483(7388):176–181.
4. Gottlieb PA, Bae C, Sachs F (2012) Gating the mechanical channel Piezo1: A comparison between whole-cell and patch recording. *Channels (Austin)* 6(4):282–289.
5. Bae C, Sachs F, Gottlieb PA (2011) The mechanosensitive ion channel Piezo1 is inhibited by the peptide GsMTx4. *Biochemistry* 50(29):6295–6300.
6. Chiang CS, Anishkin A, Sukharev S (2004) Gating of the large mechanosensitive channel in situ: Estimation of the spatial scale of the transition from channel population responses. *Biophys J* 86(5):2846–2861.
7. Sukharev SI, Sigurdson WJ, Kung C, Sachs F (1999) Energetic and spatial parameters for gating of the bacterial large conductance mechanosensitive channel, MscL. *J Gen Physiol* 113(4):525–540.
8. Bruce LJ, et al. (2005) Monovalent cation leaks in human red cells caused by single amino-acid substitutions in the transport domain of the band 3 chloride-bicarbonate exchanger, AE1. *Nat Genet* 37(11):1258–1263.
9. Gottlieb PA, Sachs F (2012) Piezo1: Properties of a cation selective mechanical channel. *Channels (Austin)* 6(4):214–219.
10. Dedman A, et al. (2009) The mechano-gated K(2P) channel TREK-1. *Eur Biophys J* 38(3):293–303.
11. Patel A, Honore E (2002) The TREK two P domain K+ channels. *J Physiol* 539(Pt 3):647.
12. Lauritzen I, et al. (2005) Cross-talk between the mechano-gated K2P channel TREK-1 and the actin cytoskeleton. *EMBO Rep* 6(7):642–648.
13. Markin VS, Sachs F (2004) Thermodynamics of mechanosensitivity. *Phys Biol* 1(1-2): 110–124.
14. Doerner JF, Febvay S, Clapham DE (2012) Controlled delivery of bioactive molecules into live cells using the bacterial mechanosensitive channel MscL. *Nature communications* 3:990.
15. Martinac B (2011) Bacterial mechanosensitive channels as a paradigm for mechanosensory transduction. *Cell Physiol Biochem* 28(6):1051–1060.
16. Moe P, Blount P (2005) Assessment of potential stimuli for mechano-dependent gating of MscL: Effects of pressure, tension, and lipid headgroups. *Biochemistry* 44(36):12239–12244.
17. Bedford MT, Richard S (2005) Arginine methylation an emerging regulator of protein function. *Mol Cell* 18(3):263–272.
18. Bedford MT, Clarke SG (2009) Protein arginine methylation in mammals: Who, what, and why. *Mol Cell* 33(1):1–13.
19. Koch-Nolte F, et al. (2006) ADP-ribosylation of membrane proteins: Unveiling the secrets of a crucial regulatory mechanism in mammalian cells. *Ann Med* 38(3): 188–199.
20. Suchyna TM, Markin VS, Sachs F (2009) Biophysics and structure of the patch and the gigaseal. *Biophys J* 97(3):738–747.
21. Barshtein G, Bergelson L, Dagan A, Gratton E, Yedgar S (1997) Membrane lipid order of human red blood cells is altered by physiological levels of hydrostatic pressure. *Am J Physiol* 272(1 Pt 2):H538–H543.
22. Hamill OP, McBride DW, Jr. (1997) Mechanogated channels in Xenopus oocytes: Different gating modes enable a channel to switch from a phasic to a tonic mechanotransducer. *Biol Bull* 192(1):121–122.
23. Bett GC, Sachs F (2000) Whole-cell mechanosensitive currents in rat ventricular myocytes activated by direct stimulation. *J Membr Biol* 173(3):255–263.
24. Dart C (2010) Lipid microdomains and the regulation of ion channel function. *J Physiol* 588(Pt 17):3169–3178.
25. Pan NC, Ma JJ, Peng HB (2012) Mechanosensitivity of nicotinic receptors. *Pflugers Arch* 464(2):193–203.
26. Suchyna TM, et al. (2004) Bilayer-dependent inhibition of mechanosensitive channels by neuroactive peptide enantiomers. *Nature* 430(6996):235–240.
27. Kim SE, Coste B, Chadha A, Cook B, Patapoutian A (2012) The role of Drosophila Piezo in mechanical nociception. *Nature* 483(7388):209–212.
28. Ostrow KL, et al. (2003) cDNA sequence and in vitro folding of GsMTx4, a specific peptide inhibitor of mechanosensitive channels. *Toxicon* 42(3):263–274.
29. Yang J, Zhang Z, Zhang XA, Luo Q (2010) A ligation-independent cloning method using nicking DNA endonuclease. *Biotechniques* 49(5):817–821.